J. Fluid Mech. (1983), *vol.* 137, *pp.* 251–272
Printed in Great Britain

Zero-crossings in turbulent signals

By K. R. SREENIVASAN,
Applied Mechanics, Yale University

A. PRABHU AND R. NARASIMHA
Indian Institute of Science, Bangalore

(Received 1 February 1982 and in revised form 1 August 1983)

A primary motivation for this work arises from the contradictory results obtained in some recent measurements of the zero-crossing frequency of turbulent fluctuations in shear flows. A systematic study of the various factors involved in zero-crossing measurements shows that the dynamic range of the signal, the discriminator characteristics, filter frequency and noise contamination have a strong bearing on the results obtained. These effects are analysed, and explicit corrections for noise contamination have been worked out. New measurements of the zero-crossing frequency N_0 have been made for the longitudinal velocity fluctuation in boundary layers and a wake, for wall shear stress in a channel, and for temperature derivatives in a heated boundary layer. All these measurements show that a zero-crossing microscale, defined as $\Lambda = (2\pi N_0)^{-1}$, is always nearly equal to the well-known Taylor microscale λ (in time). These measurements, as well as a brief analysis, show that even strong departures from Gaussianity do not necessarily yield values appreciably different from unity for the ratio Λ/λ. Further, the variation of $N_0/N_{0\max}$ across the boundary layer is found to correlate with the familiar wall and outer coordinates; the outer scaling for $N_{0\max}$ is totally inappropriate, and the inner scaling shows only a weak Reynolds-number dependence. It is also found that the distribution of the interval between successive zero-crossings can be approximated by a combination of a lognormal and an exponential, or (if the shortest intervals are ignored) even of two exponentials, one of which characterizes crossings whose duration is of the order of the wall-variable timescale ν/U_*^2, while the other characterizes crossings whose duration is of the order of the large-eddy timescale δ/U_∞. The significance of these results is discussed, and it is particularly argued that the pulse frequency of Rao, Narasimha & Badri Narayanan (1971) is appreciably less than the zero-crossing rate.

1. Introduction

For a stationary stochastic signal $y = y(x)$, Rice (1945) proved the result that the frequency N_0 of zero-crossings (with positive or negative slope) is given by

$$N_0^2 = \overline{\dot{y}^2}/4\pi^2\overline{y^2}, \tag{1.1}$$

if y and $\dot{y} \equiv \mathrm{d}y/\mathrm{d}x$ both have Gaussian distributions and are statistically independent. Liepmann (1949) gave a simpler proof of the result, and pointed out that, if y were a turbulent velocity fluctuation, measurements of N_0 could provide an independent indication of the viscous dissipation (which is proportional to

$$\overline{\dot{y}^2} = \overline{y^2}/\overline{\lambda^2}, \tag{1.2}$$

where λ is the well-known 'Taylor' microscale). In fact, it is convenient to introduce a zero-crossing (or 'Liepmann') microscale

$$\Lambda = (2\pi N_0)^{-1}, \tag{1.3}$$

and rephrase Rice's theorem as asserting the equality of the two scales ($\Lambda = \lambda$) under the stated conditions.

Later Ylvisaker (1965) proved that $\Lambda = \lambda$ for any continuous stationary Gaussian process y with finite λ without invoking statistical independence between y and $\dot{y}$.

Since turbulence is essentially non-Gaussian, Rice's result cannot *a priori* be expected to hold. However, the measurements of Liepmann, Laufer & Liepmann (1951) have shown that $\Lambda \approx \lambda$ (to within about 20%) in isotropic turbulence. The implication is that the zero-crossing scale effectively characterizes the important dynamical process of turbulence-energy dissipation. The general *a posteriori* explanation for this interesting finding of Liepmann *et al.* has been that the one-point probability density function (p.d.f.) of velocity in isotropic turbulence is not too far from being a Gaussian. What is perhaps intriguing is a similar finding (that $\Lambda \approx \lambda$) even when the one-point p.d.f.s are strongly non-Gaussian, such as for the streamwise velocity fluctuation u in a two-dimensional channel (Laufer 1950) and for wall shear-stress fluctuations in a pipe (Wetzel & Killen 1972). On this basis, one might be tempted to conclude that Rice's result has a much more general applicability than it has been proved for, but the measurements of Wygnanski & Fiedler (1969) dictate a need for some caution: these authors found that the ratio Λ/λ for u as well as the radial velocity fluctuation v varied generally between 1 and 1.5 along the centreline of an axisymmetric jet, increasing to a value as high as about 2 for v towards the edges of the jet.

More recently, Badri Narayanan, Rajagopalan & Narasimha (1974, 1977) reported extensive zero-crossing measurements of u in nearly isotropic grid turbulence and in a turbulent boundary layer. In these measurements, the zero-crossing frequency was counted visually from a trace of the signal u obtained on 35 mm film (see also §3.1). Their results suggested that, while $\Lambda/\lambda \approx 1$ in grid turbulence, the ratio in the turbulent boundary layer varied between about 3 and 5. This later result (somewhat unexpected on the basis of the balance of evidence discussed above) was attributed to the stronger departures from Gaussianity of turbulent fluctuations in the boundary layer.

While this last result tends to suggest that Λ is not a direct measure of dissipation in strongly non-Gaussian situations, further results of Badri Narayanan *et al.* emphasized the role of the zero-crossing scale in another important dynamical context. Their measurements suggested that the zero-crossing frequency N_0 of a given signal was nearly equal to the characteristic pulse frequency N_p of that signal. Pulses are simply patches of activity in a turbulent signal that has been passed through a narrow-band filter set at a sufficiently high midband frequency. Their characteristic frequency N_p was measured in these experiments with the technique of Rao, Narasimha & Badri Narayanan (1971). These high-frequency pulses have a direct bearing on the fine-structure and the internal intermittency of turbulence (e.g. Batchelor & Townsend 1949; Rao *et al.* 1971; Kuo & Corrsin 1971; Sreenivasan 1983). Two other properties of importance are attributed to the pulse frequency. First Rao *et al.* implied a connection between these pulses and the turbulent bursts observed by Kline *et al.* (1967) in the wall region of a turbulent boundary layer, suggesting that these pulses in a boundary layer are a part of the signature of a burst. Secondly Brown & Thomas (1977) showed that the pulses are coupled to the large-scale motion. There are conflicting conclusions about the relation between the pulses, bursts and

the large structure, but the connection between the high-frequency pulses and the fine-structure intermittency is almost tautological. In practice, the determination of the characteristic pulse frequency N_p is quite involved (e.g. Rao *et al.* 1971; Kuo & Corrsin 1971), and this in itself is therefore a sufficient reason for taking seriously the conclusion of Badri Narayanan *et al.* that $N_p \approx N_0$ in general; their contention was that $N_p \approx N_0$ is indeed the general result for turbulence which, in the relatively simple and degenerate case of isotropic turbulence, simplifies to $N_0 = (2\pi\Lambda)^{-1} \approx (2\pi\lambda)^{-1}$.

Essentially motivated by the new significance attributed to Λ, Antonia, Danh & Prabhu (1976) also made zero-crossing measurements electronically using a comparator and a digital counter. Their measurements included u in a variety of shear flows including the atmospheric surface layer, and the temperature fluctuation θ in a slightly heated turbulent boundary layer. They too found that the ratio $N_p/N_0 \approx 1$ for all signals (except in the atmospheric surface layer). However, in contrast with the conclusions of Badri Narayanan *et al.*, Antonia *et al.* found that $\Lambda/\lambda \approx 1$ for u even in a turbulent boundary layer.† In addition to this major difference, the data of Badri Narayanan *et al.* and Antonia *et al.*, both obtained at comparable Reynolds numbers, differ also in the value of the non-dimensional pulse frequency by a factor of 3 or 4.

Much confusion thus exists on the precise role that zero-crossings play in the physical description of turbulence. Several questions arise. Is the ratio Λ/λ substantially different from unity for strongly non-Gaussian signals? Is this ratio Reynolds-number-dependent in a turbulent boundary layer? Is $N_p/N_0 \approx 1$? What are the scaling laws for N_0 especially in the inner layer where bursting occurs? What are the implications of any of these conclusions on the outer-layer scaling proposed for the pulse frequency by Rao *et al.*? What are the sources of inconsistency among the different measurements? The goal of this paper is to answer such questions, and further explore the connection between the zero-crossings and the physical processes occurring in a turbulent shear flow. We may further note that the zero-crossings are of interest also in communication theory and in the context of signal-processing as in laser-Doppler measurements and, finally, as an approximation to the so-called 'topological entropy' (e.g. Bowen 1970) as a means of quantifying chaotic behaviours displayed by dynamical systems. The crossing frequency of levels other than zero (also considered here briefly) is of interest in such diverse contexts as agriculture, aircraft design, pollination and quality control.

The contradictory conclusions of the studies cited above clearly call for further careful measurements of zero-crossings. New measurements were carried out in two turbulent boundary layers, a two-dimensional channel and a two-dimensional wake of a circular cylinder. Section 2 describes the experimental set-up and conditions. While making these measurements, we discovered that the zero-crossing frequency can be strongly affected by a variety of factors such as the dynamic range of the signal, the filtering frequency, the signal/noise ratio, and the characteristics of the comparator (or its equivalent in visual counting). We thus undertook (§3) a detailed systematic investigation of these various factors influencing the zero-crossing measurements; corrections arising from noise contamination have also been worked out explicitly. Section 4 describes the new results; using some measurements in a heated axisymmetric jet as a reference, a major shortcoming of some of the previous data is pointed out. This section also contains a brief analysis of the ratio Λ/λ for several non-Gaussian signals. The significance of the present results is discussed in §5, which also provides a summary of the conclusions. Finally, an assessment is made in the Appendix of the accuracy attainable in the zero-crossing measurements.

† This same ratio was, however, found to be 2 for θ.

Type of flow	Signal analysed	Reynolds number	Lengthscale for the Reynolds number
Boundary layer	u	2×10^4	Boundary-layer thickness δ
	u	6.8×10^3–10^5	Boundary-layer thickness δ
Heated boundary layer	Temperature derivatives	5730	Momentum thickness θ
Wake	u	9000	Width at half-maximum defect $\hat{\delta}$
Channel	Wall stress	6000–12000	Half-width a

TABLE 1. Flows studied

2. Experimental set-up and conditions

Experiments were carried out in several flows whose brief description and salient parameters are listed in table 1. The wind tunnels used for creating these flows were standard open-circuit type, and need no further discussion. It was established that all the flows were fully developed under the conditions of measurement. The notation is as follows: U_∞ = freestream velocity, U_c = the velocity on the centreline of the channel, δ = boundary-layer thickness, a = half-width of the channel, $\hat{\delta}$ = half-defect wake thickness, ν = kinematic viscosity, $R_\delta = U_\infty \delta/\nu$, $\hat{R}_\delta = U_\infty \hat{\delta}/\nu$, $R_a = U_c a/\nu$.

Wall-shear fluctuations were obtained with a DISA miniature 55A93 probe, which is a quartz-coated nickel film deposited on the plane end of a quartz rod. The frequency response of the probe, as quoted by the manufacturer, is good up to 30 kHz.

Streamwise velocity fluctuation u was measured with single-wire probes of 5 μm and 2.5 μm diameter Pt–Rh wire. They were operated on a constant-temperature anemometer whose response was flat up to 15 kHz. The differentiator had a linear response up to 15 kHz. A block diagram of the signal-processing equipment is given in figure 1. In some of the measurements, the probes were operated on a DISA 55M01 constant-temperature anemometer. The signals were linearized (through a DISA 55D10 linearizer) and passed through a 55D26 signal conditioner before being recorded on a Hewlett-Packard 3960A FM tape recorder, whose −3 dB upper cut-off frequency was 6.3 kHz. Zero-crossings were obtained by first removing the d.c. of the signal with a Krohn–Hite filter (cut-off at 0.02 Hz) and then passing the output through a Digital Electronics comparator (with the comparator level grounded) and a digital frequency meter. The zero-crossing frequency was obtained not only using tape-recorded signals but also directly *in situ*. The tape-recorded signals were generally processed as described above; but, in some cases, the zero-crossing frequency was obtained directly on a PDP 11/45 computer instead of a frequency meter. Here, the signals were pre-filtered at the estimated Kolmogorov frequency f_η and then were digitized at $2f_\eta$ on a 10 bit (including sign) A/D converter. The probability density function of the interval between successive zero-crossings was obtained (as a rule) on the digital computer. On occasions, this was checked by obtaining a fairly long trace (about 20 sec) of the signal on photographic paper and computing the distribution by straightforward counting.

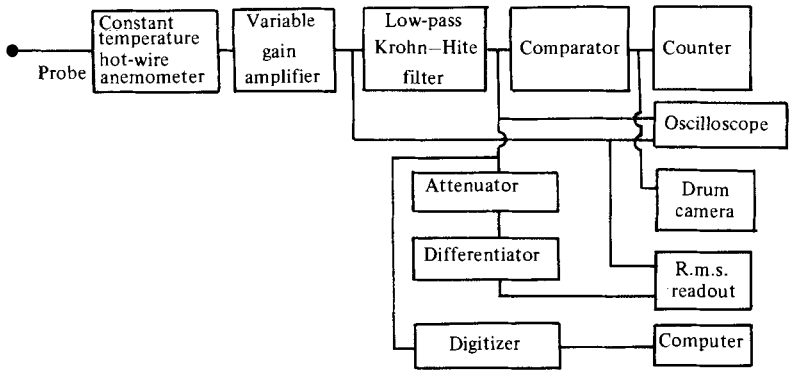

FIGURE 1. Block diagram of signal-processing equipment.

3. Factors influencing zero-crossing measurements

3.1. *Dynamic range of the signal*

Figure 2 gives the circuit diagram of the comparator used here. It consists essentially of an open-loop op-amp differential amplifier with transistor clippings at the output. The two outputs are complementary to each other, with the normal output being high when the input voltage is greater than the reference voltage, which can be varied at will.

Figure 3 shows a typical random signal and the corresponding normal output from an ideal comparator and the actual one. The two outputs differ for the following reasons. (*a*) When the reference voltage is zero the real output is high only when the signal voltage is higher than a small non-zero d.c. bias voltage (positive or negative), which is the product of the offset bias current at the input and the difference in resistance between the two input resistors of the op-amp. This small bias voltage could in principle be corrected for by adjusting the reference voltage suitably. (*b*) Because of the finite open-loop gain of the op-amp, there exists a region called the dead band, such that only when the signal level crosses this dead band will the output of the op-amp be sufficiently large to trigger the transistor (see figure 2); only then is the output of the comparator high. The width of this dead band increases with frequency since the open loop gain of the op-amp decreases with the increase in frequency. To minimize this error, it is therefore necessary to amplify the signal so that the ratio of the dead band to the signal amplitude is sufficiently small.

Figure 4 shows the effect on N_0 of the gain G of the system through which the signal is processed. At low signal amplitudes, there will be many 'runs' (a term in common statistical usage (see e.g. Feller 1950) which we adopt to indicate the signal between two successive zero-crossings) which are masked within the dead band. There will in principle always be some such runs no matter what the gain, but they will become fewer and fewer with increasing gain and the true value is approached from below when the gain is sufficiently high.

To obtain an appreciation of the numbers involved, consider the following argument for a dead band B which we shall consider (for simplicity) to be independent of frequency. If $p(y, \dot{y})$ represents the joint probability density of y and $\dot{y}$, then Rice showed that the number of times $N(\xi)$ that a given signal crosses the level ξ is given by

$$N(\xi) = \int_{-\infty}^{\infty} |\dot{y}|\, p(\xi, \dot{y})\, \mathrm{d}\dot{y}. \tag{3.1}$$

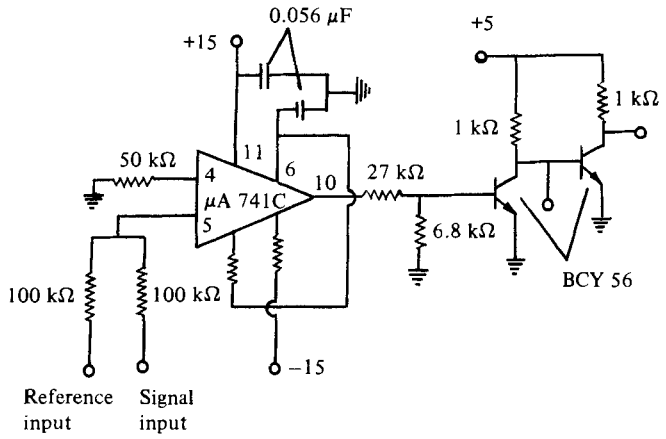

FIGURE 2. Circuit diagram of the comparator.

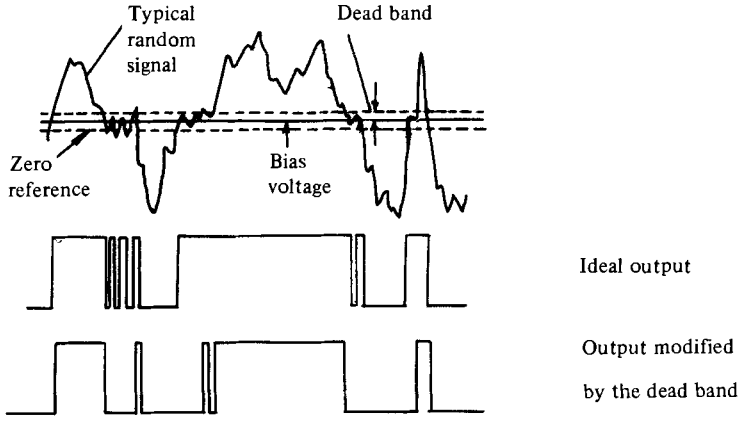

FIGURE 3. A typical random signal and the effect of dead band.

If y and $\dot{y}$ are statistically independent, (3.1) can be manipulated to write

$$\frac{N(\xi)}{N_0} = \frac{p_{\dot{y}}(\xi)}{p_{\dot{y}}(0)}, \quad N_0 \equiv N(0). \tag{3.2}$$

Measurements show that this relation is adequately satisfied for 'white' noise from a commercial random-noise generator whose measured p.d.f. is Gaussian to a good approximation, as well as for the evidently non-Gaussian wall shear-stress fluctuation (figure 5).

It follows from (3.2) that the fractional error $\epsilon = (N_0 - N(B))/N_0$ is given by

$$\epsilon = \frac{p_{\dot{y}}(0) - p_{\dot{y}}(B)}{p_{\dot{y}}(0)}. \tag{3.3}$$

For a Gaussian process with $p_y(y) \sim e^{-\frac{1}{2}y^2}$ we find by inverting (3.3) that to achieve $\epsilon = 0.2$ (i.e. 20% accuracy in the zero-crossing frequency) we must have $B \approx 0.7 \times$ r.m.s. value of the signal. In typical experimental situations here, $B \approx 7$ mV, and so the signal must be amplified to an r.m.s. value of at least 10 mV. A more stringent demand (for instance) that $\epsilon = 0.02$ requires that the r.m.s. value of the

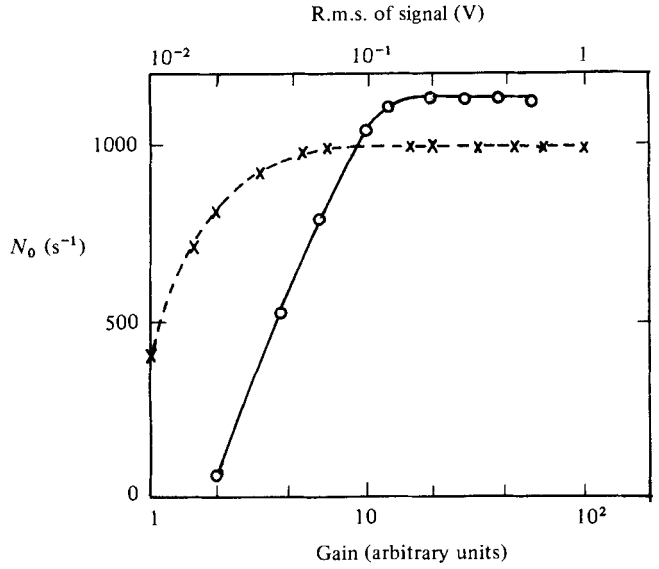

FIGURE 4. Effect of system gain on the number of zero-crossings: ○, wall shear-stress fluctuations, $R_a = 11.5 \times 10^3$; ×, white noise.

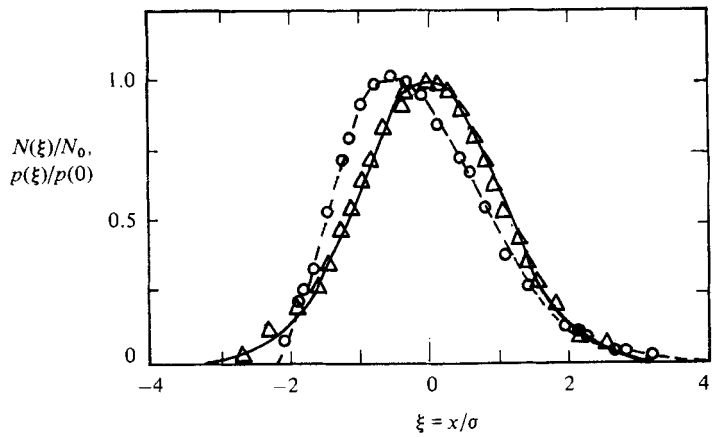

FIGURE 5. Variation with threshold setting of the zero-crossing frequency, compared with the amplitude probability density function; see (3.2). ξ = threshold setting in units of the r.m.s. value of the signal. Measured $p(\xi)/p(0)$: ——, Gaussian; – – –, wall shear-stress fluctuation. Measured $N(\xi)/N_0$: △, white noise; ○, wall shear-stress fluctuation.

signal must be at least 25 mV. Actually the gains required are somewhat higher than these estimates show, because of the frequency dependence of the dead band.

In order to obtain similar estimates for any other quantity whose p.d.f. is not known analytically, it is clear that (3.3) can be inverted only with the help of an empirical fit to the measured p.d.f. For u in the viscous sublayer of a turbulent boundary layer (say at $y^+ \approx 2$) using the measured probability density function of Gupta & Kaplan (1972), we require that the r.m.s. values of the signal must be at least 20 mV ($\approx 3B$) and 50 mV ($\approx 7B$) respectively for $\epsilon = 0.2$ and 0.02.

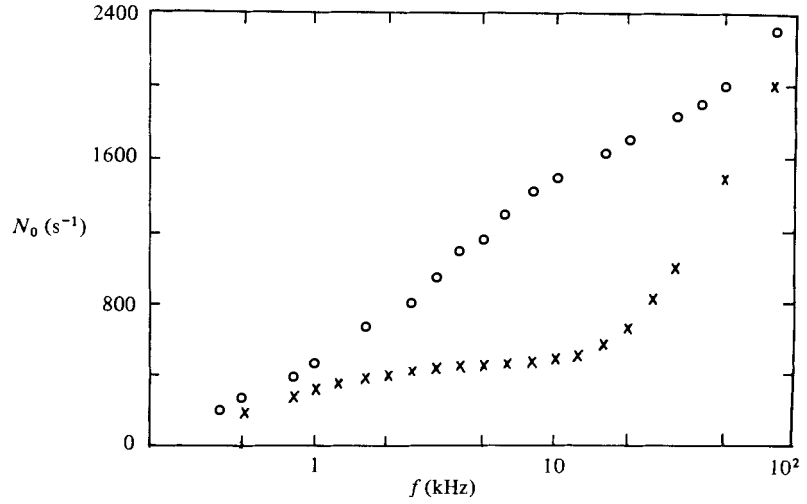

FIGURE 6. Variation of N_0 with the cut-off frequency: O, poor signal-to-noise ratio; ×, reasonably good signal-to-noise ratio.

3.2. *Frequency cut-off and noise*

It is clear that the measured zero-crossing frequency will be influenced significantly by the high-frequency content of the signal. If the signal is passed through a low-pass filter set at the frequency f_1, it is to be expected that the zero-crossing frequency increases initially with f_1 (this increase being linear for white noise) and then attains a plateau, representing the true value. Further increase in the value of f_1 increases the noise content; therefore at substantially higher settings of f_1, the number of crossings starts increasing again: illustrative experimental data are shown in figure 6.

If the signal-to-noise ratio is low, so that the 'gap' between the high-frequency content of the signal and the noise is small, the plateau region diminishes in extent. Even if the noise is marginally higher than is acceptable in many cases, this plateau may disappear completely (figure 6). Under these conditions, it is not possible to obtain the correct crossing frequency simply by setting the filter to a certain cut-off value. It is thus useful to consider the problem of explicit noise correction in more detail.

3.3. *Corrections to N_0 for noise contamination*

It is reasonable to assume that the signal/noise ratio is large and that the signal and noise are statistically independent.

Let

$$y = s+n, \tag{3.4}$$

where s is the signal and n the noise.† Then the joint probability density $p_y(y, \dot{y})$ can be written as a convolution of the joint probability densities $p_s(s, \dot{s})$ and $p_n(n, \dot{n})$:

$$p_y(y, \dot{y}) = \int_{-\infty}^{\infty} p_s\{(y-n), (\dot{y}-\dot{n})\}\, p_n(n, \dot{n})\, \mathrm{d}n\, \mathrm{d}\dot{n}. \tag{3.5}$$

† Here and elsewhere in this paper, to avoid unnecessary symbols, we have used the same symbol for the random variable as well as the possible value in probability space which that function can take.

Expanding $p_s\{(y-n), (\dot{y}-\dot{n})\}$ in Taylor series around $(y, \dot{y})$ and retaining only terms up to second order, we get

$$p_s\{(y-n),(\dot{y}-\dot{n})\} = p_y(y,\dot{y}) - n\frac{\partial p_s}{\partial y}\bigg|_{n=0} - \dot{n}\frac{\partial p_s}{\partial \dot{y}}\bigg|_{\dot{n}=0} + \frac{n^2}{2}\frac{\partial^2 p_s}{\partial y^2}\bigg|_{n=0} + \frac{\dot{n}^2}{2}\frac{\partial^2 p_s}{\partial \dot{y}^2}\bigg|_{\dot{n}=0} + n\dot{n}\frac{\partial^2 p_s}{\partial y\,\partial \dot{y}}\bigg|_{n=0,\,\dot{n}=0}. \quad (3.6)$$

Using (3.6) in (3.5), evaluating the integrals with respect to n and $\dot{n}$ and noting that the mean values of n and $\dot{n}$ are zero (which implies that $\overline{n\dot{n}} = 0$ if n and $\dot{n}$ are independent), we get

$$p_y(y,\dot{y}) = p_s(y,\dot{y}) + \frac{\overline{n^2}}{2}\frac{\partial^2 p_s}{\partial y^2}\bigg|_{n=0} + \frac{\overline{\dot{n}^2}}{2}\frac{\partial^2 p_s}{\partial \dot{y}^2}\bigg|_{\dot{n}=0}. \quad (3.7)$$

Using (3.7) in (3.1) we get the level-crossing rate as

$$N_y(\xi) = N_s(\xi) + \frac{\overline{n^2}}{2}\int_{-\infty}^{\infty} |\dot{y}|\frac{\partial^2 p_s}{\partial y^2}\bigg|_{n=0} d\dot{y} + \frac{\overline{\dot{n}^2}}{2}\int_{-\infty}^{\infty} |\dot{y}|\frac{\partial^2 p_s}{\partial \dot{y}^2}\bigg|_{\dot{n}=0} d\dot{y}. \quad (3.8)$$

Taking the differentiation outside the integral in the second term on the right-hand side of (3.8), integrating the third term by parts, and simplifying, we get

$$\begin{aligned} N_y(\xi) &= N_s(\xi) + \frac{\overline{n^2}}{2}\frac{\partial^2 N_s(\xi)}{\partial \xi^2} + 2\frac{\overline{\dot{n}^2}}{2}p_s(\xi,0) \\ &= N_s(0)\left[g + \frac{\overline{n^2}}{2\overline{s^2}}\frac{\partial^2 g}{\partial \eta^2} + \frac{\overline{\dot{n}^2}}{\overline{\dot{s}^2}}\frac{\Lambda_s}{\lambda_s}P_s(\eta,0)\right], \end{aligned} \quad (3.9)$$

where

$$\left.\begin{aligned} \eta &= \frac{\xi}{(\overline{s^2})^{\frac{1}{2}}}, \quad g = \frac{N_s(\xi)}{N_s(0)}, \quad P_s = 2\pi(\overline{s^2})^{\frac{1}{2}}(\overline{\dot{s}^2})^{\frac{1}{2}}p_s, \\ \Lambda_s &= (2\pi N_s(0))^{-1}, \quad \lambda_s = \frac{(\overline{\dot{s}^2})^{\frac{1}{2}}}{(\overline{s^2})^{\frac{1}{2}}}. \end{aligned}\right\} \quad (3.10)$$

In particular, at $\xi = 0$,

$$N_y(0) = N_s(0)\left[1 + \frac{\overline{n^2}}{2\overline{s^2}} + \frac{\overline{\dot{n}^2}}{\overline{\dot{s}^2}}\frac{\Lambda_s}{\lambda_s}P_s(0,0)\right], \quad (3.11)$$

which expresses the measured zero-crossing rate in terms of the true value corresponding to the signal. In many situations, the correction due to the third term in (3.11) is larger than that due to the second, because white noise (with a flat spectral density) has a relatively high mean-square derivative.

To demonstrate the effectiveness of these calculations, measurements were made in a boundary layer with a 5 μm diameter hot wire, which gives a generally noisier signal than that observed with the usual 2.5 μm diameter wire. Figure 7(*a*) shows the zero-crossing frequency plotted as a function of the gain and cut-off frequency. As mentioned in §3.1, this frequency does not attain a final asymptotic value either with respect to the gain of the system or the cut-off frequency.

An iteration is in principle required in using (3.11), but, if the noise is not too large, it is often possible to use the Λ and λ corresponding to signal plus noise instead of for the signal alone. Such was the case for present measurements. Figure 7(*b*) shows that, when the data are corrected for noise according to (3.11), there is a value of N_0 which remains reasonably independent of the gain as well as the cut-off frequency. Noise was measured by operating the hot wire in the freestream at a wind-tunnel speed equal to that at the measuring station within the boundary layer.

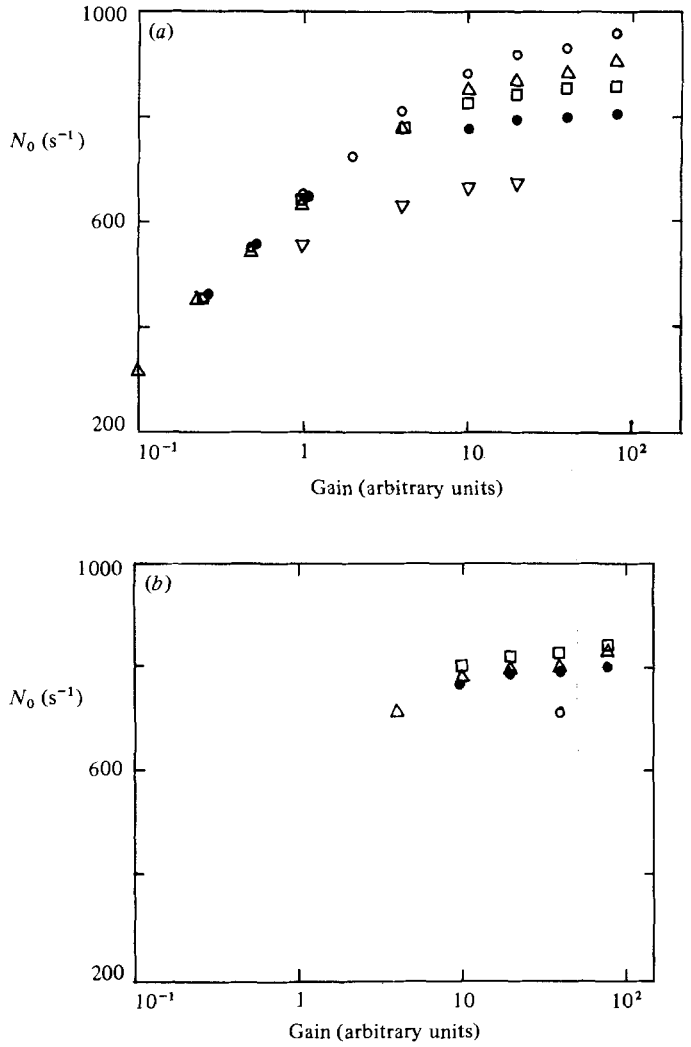

FIGURE 7 (*a*, *b*). For caption see facing page.

3.4. *Correction to the Taylor microscale*

From (3.4), and noting that s and n are independent, one gets

$$\overline{\dot{y}^2} = \overline{\dot{s}^2} + \overline{\dot{n}^2};$$

hence

$$\frac{\lambda_y^2}{\lambda_s^2} = 1 + \frac{1}{r^2}\left(1 - \frac{\lambda_y^2}{\lambda_n^2}\right), \tag{3.12}$$

where $r = (\overline{s^2}/\overline{n^2})^{\frac{1}{2}}$ is the signal-to-noise ratio. Figure 7 (*c*) shows measurements of the time derivatives of the noise as well as the signal representing the streamwise velocity fluctuations at the centre of a plane wake. When corrected for noise according to (3.12), the mean-square derivative of u is seen to be reasonably independent of the cut-off frequency above 2 kHz.

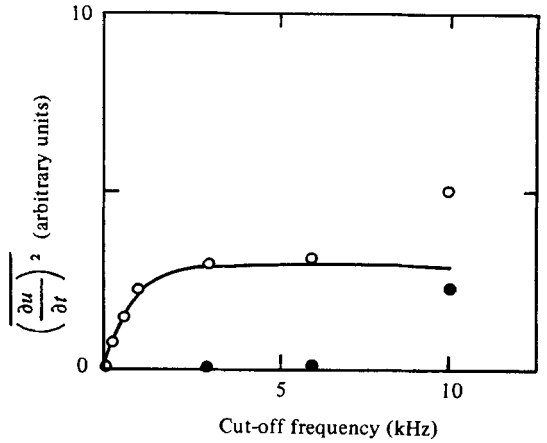

FIGURE 7. (*a*) Variation of N_0 with the gain and cut-off frequency (with no correction for noise) in a two-dimensional boundary layer. $U = 12$ m/s, $R_\delta \approx 2 \times 10^4$, $y/\delta \approx 0.1$. Cut-off frequency in kHz: ▽, 2; ●, 4; □, 6; △, 10; ○, 15. (*b*) Data of (*a*) corrected for noise. Legend same as in figure 7(*a*). N_0 does not reach its asymptotic value at 2 kHz cut-off frequency and hence those points are not shown. The comparator would not be measuring all the zero-crossings at 15 kHz cut-off frequency with gain at 70; hence the correction for noise brings the point appreciably below the true value as shown. (*c*) Variation with the cut-off frequency of the mean-square derivative of the signal, noise and the sum: ●, noise, ○, signal + noise; ——, corrected for noise. Signal is u in a turbulent wake.

4. Results

4.1. *The ratio of the two microscales*

Figure 8 shows the ratio Λ/λ for different signals in different flows. (For a discussion of the accuracy of the present results see the Appendix.) Clearly, $\Lambda \approx \lambda$ in all the flows investigated here. In these measurements, the precautions previously mentioned in §3 were observed. In particular, both the gain and the cut-off frequency were appropriate to the respective plateau regions discussed in §§3.1 and 3.2. Corrections for noise were also made. It is probably worth emphasizing the result from figure 8(*d*) which shows that $\Lambda/\lambda \approx 1$ also for strongly non-Gaussian signals such as the temperature derivatives in a slightly heated turbulent boundary layer. (For a description of how the derivatives were measured, reference should be made to Sreenivasan, Antonia & Danh (1977).)

We thus suspected that the previous results leading to contrary conclusions arose directly from experimental errors in measuring the zero-crossing frequency and/or the Taylor microscale. With this in mind, we particularly examined in detail the method employed by Badri Narayanan *et al.* (1974, 1977). These authors passed their signals through a splitter which gives only one half of the signal (above or below the mean). The split signal was then displayed with zero sweep on an oscilloscope screen and photographed on 35 mm film using a drum camera. The number of runs was then counted visually.

In this technique, an effective dead band can arise in two ways. First, the electronic dead band discussed in connection with the comparator is equally relevant to the splitter, which would not be triggered by a certain number of runs at low amplitude. Secondly, the finite thickness of the trace of the photographed signal can act as an effective dead band. The typical height of the photographed film was about 10 mm from the mean of the signal to the largest amplitude recorded on the film (called the peak of the signal for convenience), and the thickness of the base line varied

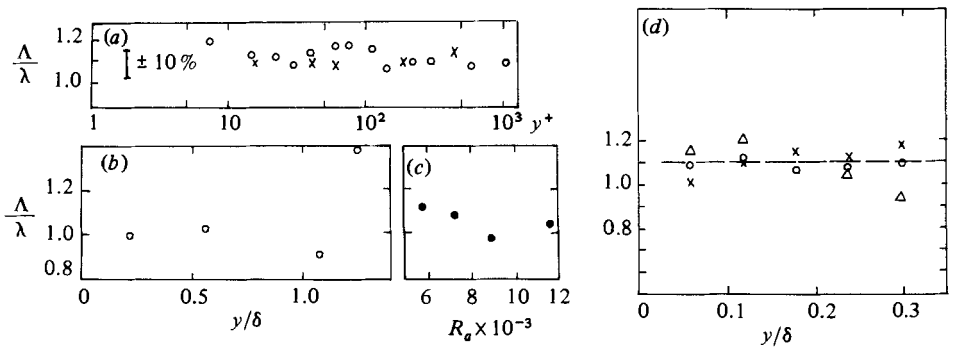

FIGURE 8. The ratio Λ/λ. (*a*) u, boundary layer; ○, $R_\delta \approx 4.9 \times 10^4$; ×, 2×10^4. (*b*) u, wake; $\hat{R}_\delta \approx 9 \times 10^3$. (*c*) Wall shear-stress fluctuations in a channel flow. (*d*) $\partial\theta/\partial x$ (△), $\partial\theta/\partial y$ (○), $\partial\theta/\partial z$ (×) in a heated turbulent boundary layer, $R_\theta \approx 5730$.

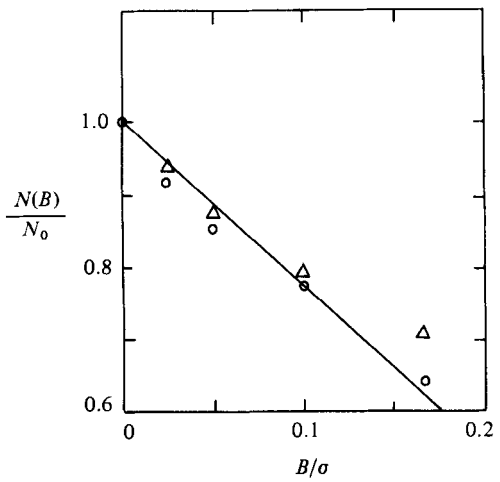

FIGURE 9. Ratio of band-crossings to the zero-crossings in a slightly heated boundary layer; $y/\delta \approx 0.15$, $R_\delta \approx 5 \times 10^4$: ○, U; △, T.

between 0.5 mm and (occasionally) 1 mm. Assuming a peak/r.m.s. ratio of about 5, this amounts to a dead band whose effective half-width varied between 0.25 and 0.5 of the r.m.s. value of the signal. Visual counting under these conditions would be equivalent, in some sense, to counting not the crossing rate of the mean of the signal, but that of a small band on either side of the mean. An estimate of the effect of this dead band on the crossing rate was obtained on a digital computer. If y_j represents the jth digital sample of the signal y with zero mean, then a zero-crossing can be said to have occurred if the product $y_j y_{j+1} < 0$. Extending this definition, a band-crossing can be said to have occurred if, in addition, $|y_j| < B$, $|y_{j+1}| > B$, where B is the half-bandwidth. Figure 9 gives the ratio of the band crossing to the zero-crossing frequency† as a function of the ratio of the half-bandwidth to the r.m.s. value σ of the signal. It appears from figure 9 that, with B/σ in the range 0.25–0.5, there would be a serious underestimate of the zero-crossing frequency in such a technique.

† Note that this ratio is slightly different for different signals. The peakier the probability density at $y = 0$ of y, the faster is the rate of decrease of $N(B)/N_0$ with B.

Further, a dependence of the zero-crossing rate on the film speed is also likely in these experiments. Low film speeds result in further compressing the length of smaller runs on the film; if the runs are of small amplitudes as well, they are likely to be missed, thus resulting in a further underestimate of N_0. A similar effect is likely to be present even when signals are recorded on tape and processed; for example, when the signal representing wall shear-stress fluctuations in the channel flow is played back into the electronic counting system at a tape speed of 38.1 cm s^{-1}, the resulting count was 7 and 8 % less than that when played back at speeds of 9.53 cm s^{-1} and 2.38 cm s^{-1} respectively, all other conditions being the same. At slower tape speeds, the apparent frequency of the signal fed into the comparator will decrease, thus effectively decreasing the dead band of the comparator for a given real-time frequency.

4.2. *A brief analysis of non-Gaussian signals*

One conclusion that follows from the present measurements is that $\Lambda/\lambda \approx 1$ even when drastic departures from Gaussianity occur. This seemed worth further examination. From the definition of Λ and λ, a minor manipulation of Rice's expression yields, under the assumptions leading to (3.2),

$$\frac{\Lambda}{\lambda} = \left[\frac{\int_{-\infty}^{\infty} y^2 p_y(y)\,\mathrm{d}y}{\int_{-\infty}^{\infty} \dot{y}^2 p_{\dot{y}}(\dot{y})\,\mathrm{d}\dot{y}}\right]^{\frac{1}{2}} 2\pi p_y(0)\left\{\int_{-\infty}^{\infty} \dot{y} p_{\dot{y}}(\dot{y})\,\mathrm{d}\dot{y}\right\}^{-1}, \tag{4.1}$$

which seems to suggest a complicated dependence of the ratio Λ/λ on p_y and $p_{\dot{y}}$. However, we have already seen that the details of p_y and $p_{\dot{y}}$ are not critical for the ratio Λ/λ. As a further example, consider the deterministic case of the sine wave $y = a\sin\omega t$. Obviously p_y and $p_{\dot{y}}$ are both non-Gaussian. Here $\Lambda = (2\pi N_0)^{-1} = \omega^{-1}$, and $\lambda = a\sin\omega t/\omega a\cos\omega t = \omega^{-1}$, so that $\Lambda = \lambda$. The result is true also for an intermittent signal such as a half-rectified sine wave.

Table 2 summarizes the calculations using (4.1) and measurements made with various types of signals and probability density functions.† These results show that the ratio Λ/λ is close to unity in a large number of cases irrespective of the precise form of p_y. Sizeable departures from unity cannot, however, be ruled out, as in the case of triangular signal where the ratio Λ/λ depends on the factor l_1/l_2;‡ even here, however, Λ/λ varies only by a factor 5 when l_1/l_2 varies a hundredfold (from 1 to 100), with the accompanying drastic changes in $p_{\dot{y}}$. *It is thus quite clear that Gaussianity is not the limiting factor for the result $\Lambda = \lambda$ to hold approximately.* The critical factor is something else, unknown at the present.

4.3. *Inner- and outer-layer similarity*

The variation of the zero-crossing frequency N_0 across the boundary layer is shown in figures 10(*a*, *b*). In the wall region, N_0 increases with the normal distance y, reaches a maximum value $N_{0\max}$ approximately at the outer edge of the logarithmic region, and decreases in the outer region (by about 20 % of $N_{0\max}$). It is of interest to note that $N_0/N_{0\max}$ appears to be independent of Reynolds number in the inner layer

† Many other more complicated combinations of p_y and $p_{\dot{y}}$ were tried with the same results, but these are not given here because their relation to turbulence is not clear.

‡ The limits $l_1/l_2 \to 0$ or ∞ are to be excluded because $\lambda = 0$ in these limits, thus violating Ylvisaker's (1965) condition.

y, signal	$p(y)$	$p(\dot{y})$	$\frac{\Lambda}{\lambda}$ according to (4.1)	Experimental result†	Remarks
Random noise	Gaussian	—	1	1.035 (6)	Random noise with different spectral content were tried, with the same result
Squared random noise (0–4 kHz)	—	—	—	1.031 (6)	—
Squared random noise (200–400 Hz)	—	—	—	1.186 (5)	—
$a \sin \omega t$	—	—	—	1.0 (6)	$a \sin^2 \omega t$ also gives the same result
	$\alpha e^{-\alpha y}$ $(0 \leqslant y < \infty)$	$\beta e^{-\beta y}$ $(-\infty < \dot{y} \leqslant 0)$	$e^2/2\pi = 1.176$		
	Top-hat	Ramp	$\frac{81}{16\pi}\sqrt{\frac{2}{3}} = 1.316$		
	Ramp	Top-hat	$\left(\frac{3}{2}\right)^{\frac{1}{2}}\frac{3}{\pi} = 1.170$		
	Top-hat	Top-hat	$4/\pi = 1.273$		
	Ramp	Ramp	1.208		
	$\frac{1}{2\pi\sigma_y}\exp\left[-\frac{y^2}{2\sigma_y^2}\right]$ $(-\infty < y < \infty)$	$\alpha \exp(-\alpha\dot{y})$ $(0 \leqslant \dot{y} < \infty)$	$\frac{e}{(2\pi)^{\frac{1}{2}}} = 1.084$		
	$\beta \exp(-\beta y)$ $(0 < y < \infty)$	$\frac{1}{2\pi\sigma_{\dot{y}}}\exp\left(-\frac{\dot{y}^2}{2\sigma_{\dot{y}}^2}\right)$ $(-\infty < \dot{y} < \infty)$	$\frac{e}{(2\pi)^{\frac{1}{2}}} = 1.084$		
Triangular wave $y = (h/l_1)t$, for $t < l_1$ $= h-(h/l_2)(t-l_1)$, for $l_1 \leqslant t \leqslant l_1+l_2$	hat	$\frac{l_2}{l_1+l_2}\delta\left(-\frac{h}{l_1}\right)+\frac{l_1}{l_1+l_2}\delta\left(\frac{h}{l_2}\right)$	$\frac{\sqrt{3}}{\pi}\left(\frac{l_1}{l_2}+\frac{l_2}{l_1}\right)$ $= 1.103$ if $l_1 = l_2$	1.1 when $l_1 = l_2$	If $l_1 = l_2$, y^2 gives the result 1.196 (3)

† The number in parentheses indicates the number of trials made with different conditions of amplitude, frequency, crest of peak ratio, etc.

TABLE 2. The ratio of zero-crossing to Taylor microscale for various probability distributions of the signal and its derivative. A probability density p that is constant between two values of the variable and vanishes elsewhere is called a hat; one that varies linearly from zero between two values of the variable, and vanishes elsewhere, is called a ramp.

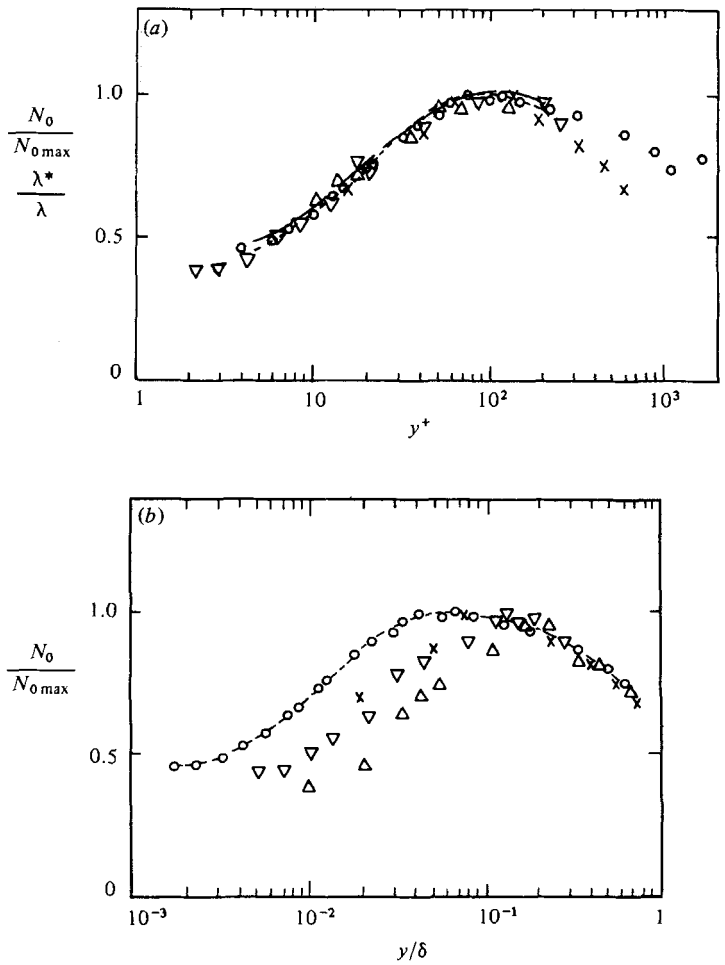

FIGURE 10. (*a*) Inner-layer similarity of the distribution of zero-crossing frequency, $N_0/N_{0\max}$: △, $R_\delta = 6.8\times10^3$; ▽, 8.5×10^3; ×, 2×10^4; ○, 4.9×10^4. λ^*/λ from measurements of Ueda & Hinze (1975): ——, $R_\delta = 3.6\times10^4$; – – –, 1.2×10^4. (*b*) Outer-layer similarity of the distribution of zero-crossing frequency, $N_0/N_{0\max}$. Legend (where applicable) as in (*a*).

(figure 10*a*)† when plotted against y^+, and in the outer layer (figure 10*b*) when plotted against y/δ. This result is consistent with the familiar notion that there are essentially two similarity laws in a turbulent boundary layer.

Using now the result that $\Lambda/\lambda \approx 1$, one can also plot the Taylor microscale data in the form $\lambda^*/\lambda(y)$ (where $\lambda^* = \lambda_{\max}^{-1}$) as a further test of the inner-layer similarity. Data on this ratio evaluated from the measurements of Ueda & Hinze (1975) in the turbulent boundary layer at two Reynolds numbers are also shown in figure 10(*a*). The agreement with the zero-crossing data is excellent.

† Measurements of Badri Narayanan *et al.* (1977) also show a drop in the crossing frequency towards the wall. If their crossing frequency at various y^+ were affected by the same *relative* error, it is likely that their data are also consistent with this similarity. A quantitative confirmation of this possibility cannot unfortunately be made because it is not possible to recover their data in the raw form.

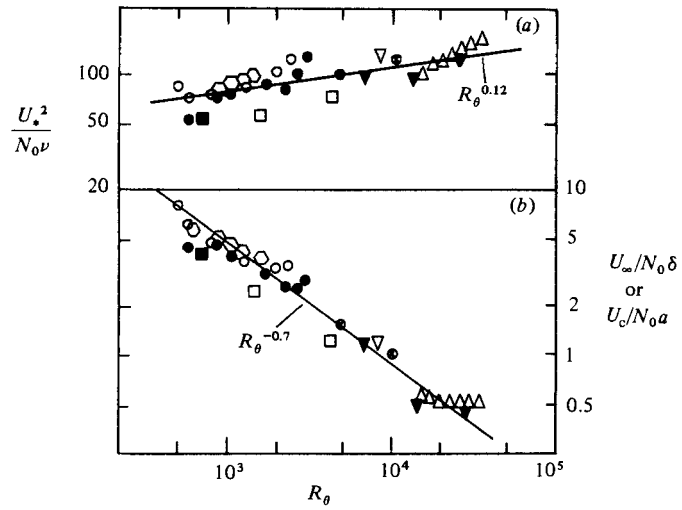

FIGURE 11. (*a*) Inner scaling for the zero-crossing frequency. Zero-crossings directly measured: △, Wetzel & Killen (1972), pipe; ○, ●, Repik & Sosedko (1976), boundary layer; ×, present, channel; ⊗, present, boundary layer. Inferred from microscale measurements: ▽, Klebanoff (1955), boundary layer; ▽, Comte-Bellot (1962), channel; □, Ueda & Hinze (1975), boundary layer; ■, Bakewell & Lumley (1976), pipe. (*b*) Outer scaling for the zero-crossings. Symbols as in (*a*).

4.4. *Scaling laws for* $N_{0\max}$

4.4.1. *Inner layer*

The scaling laws for $N_{0\max}$ remain to be determined. The inner and outer similarities of figures 10(*a*, *b*) when normalized by $N_{0\max}$ suggest that it is enough to determine the scaling laws for N_0 at a fixed y^+ in the inner layer, or a fixed y/δ in the outer layer. Because of the possible connection implied by the previous investigators between N_0, N_p and bursts in the inner layer, we concentrated more on the inner layer. We first note that the zero-crossing frequency is sensibly independent of y^+ for $y^+ \lesssim 3$ (as seen, for example, from the inverted triangles of figure 10*a*). From measurements at two Reynolds numbers, Ueda & Hinze (1975) inferred that $\bar{\lambda}^+ \approx 3.1y^+$ for small y^+, where $\bar{\lambda} = U\lambda$ is the spatial microscale (assuming Taylor's hypothesis to be valid). This implies that $U_*^2/N_0\nu$ is a constant independent of Reynolds number. Several measurements of N_0 for $y^+ \leqslant 3$ are plotted in figure 11(*a*). Assuming that the inner-layer scaling in turbulent boundary layers, channels and pipes are essentially the same, and further that $\Lambda = \lambda$, the data inferred from microscale measurements of other sources are also plotted in the figure. The scatter in the data does not permit an unambiguous fit, but a slight dependence upon the Reynolds number is unmistakable. A possible fit to the data is

$$\frac{U_*^2}{N_0\nu} \approx 36R_\theta^{0.12}. \tag{4.2}$$

This slight Reynolds-number dependence cannot be attributed only to experimental uncertainties, and will be commented upon in §5.

The outer scaling clearly does not apply (figure 11*b*). Again, a possible fit to the data is

$$\left.\begin{matrix} U_\infty/N_0\delta \\ U_c/N_0 a \end{matrix}\right\} \approx 510R_\theta^{-0.70}. \tag{4.3}$$

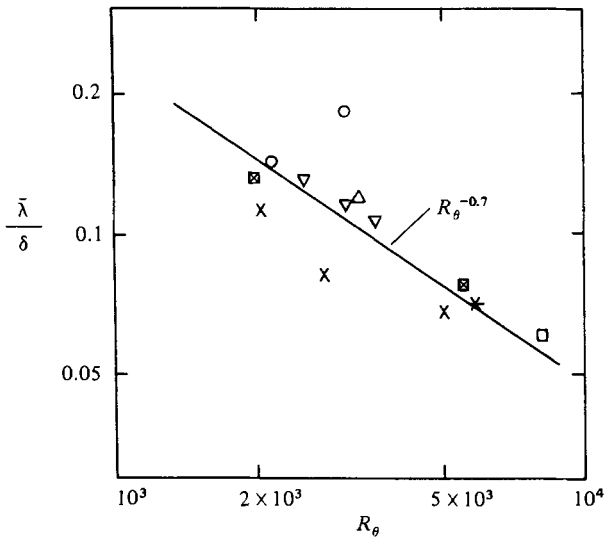

FIGURE 12. Variation of $\bar{\lambda}/\delta$ with Reynolds number; $y/\delta \approx 0.75$: ∇, Townsend (1951); $\square$, Klebanoff (1955); $\triangle$, Blackwelder & Kovasznay (1970); $\bigcirc$, Antonia (1973) $\divideontimes$, Antonia *et al.* (1976); $\times$, Badri Narayanan *et al.* (1977); $\boxtimes$, present.

4.4.2. *Outer layer*

If $\Lambda = \lambda$, it follows that

$$\frac{U_\infty}{N_0 \delta} \approx 2\pi \frac{\bar{\lambda}}{\delta} \frac{U_\infty}{U}.$$

Noting that U_∞/U is not a strong function of Reynolds number for fixed y/δ in the outer layer, it follows that

$$\frac{U_\infty}{N_0 \delta} \sim \frac{\bar{\lambda}}{\delta}.$$

In the outer layer, $\bar{\lambda}/\delta$ increases monotonically with y for $y/\delta \lesssim 0.5$, and does not vary a great deal for $y/\delta \gtrsim 0.5$. In the latter region (typically $y/\delta \approx 0.75$), experimental data from several sources (figure 12) show that the fit

$$\frac{\bar{\lambda}}{\delta} \sim R_\theta^{-0.7} \tag{4.4}$$

is not unreasonable (though a somewhat weaker dependence is perhaps preferable), thus showing general consistency with (4.3). Notice that the scatter in the data for this seemingly simple parameter is considerable, again not surprising in view of the significant influence of noise on λ (see figure 7*c*).

4.5. *Distribution of interval between successive zero-crossings*

Consider now the distribution of the interval l between successive zero-crossings. The theoretical treatment of this problem (see e.g. Rice 1945; Longuet-Higgins 1958) is still incomplete. Under certain assumptions, Rice showed that, in the limit $l \to 0$, the probability density of l is proportional to l itself. Longuet-Higgins worked out the general asymptotic cases, but these are sufficiently complicated that a simple approximation, even if only empirical, is useful. For large l, it is plausible, as Rice

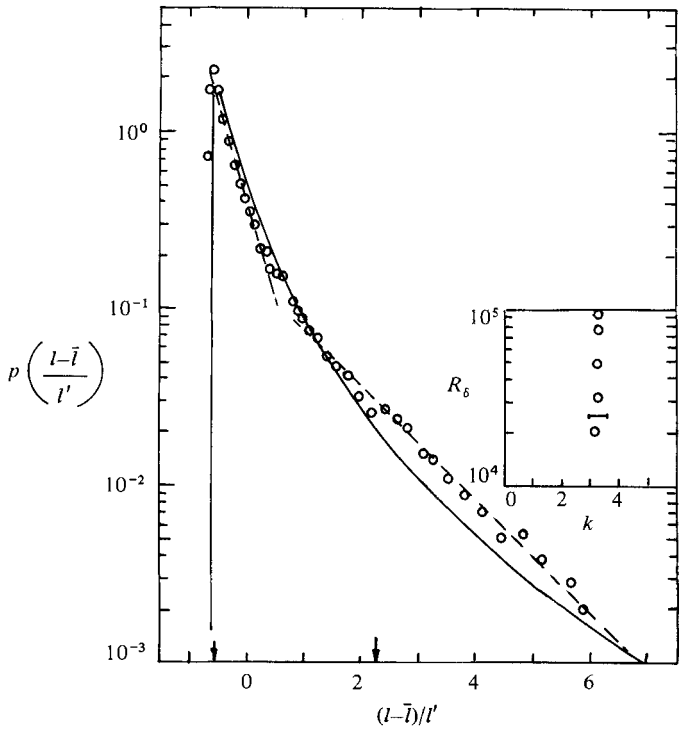

FIGURE 13. Probability density of the interval l between successive zero-crossings in the logarithmic region of a turbulent boundary layer; $R_\delta \approx 4.9 \times 10^4$; number of samples 16700: ---, exponential approximations; ——, lognormal density with same mean and variance for l as the measured values. The inset shows the variation of slope of the exponential tail with Reynolds number.

pointed out, that the probability of occurrence of a zero-crossing is independent of the preceding one, so that the process is of the Poisson type. In fact, Longuet-Higgins quotes Kuznetsov, Stratonovich & Tiknonov (1954) as having derived an exponential law for $p(l)$ when l is large. No simple theory exists for intervals of intermediate length.

Figure 13 shows the normalized probability density of the interval between successive zero-crossings. Here $\bar{l}$ = mean value of l, l' = r.m.s. value of l. For $l-\bar{l} \gtrsim 1.2l'$ the distribution can be approximated by an exponential

$$p(l) \propto \exp\left(-\frac{l-\bar{l}}{kl'}\right),$$

where k is a constant. It is interesting to note that there is a significant region of small l ($-0.5l' \lesssim l-\bar{l} \lesssim 0.5l'$) over which another exponential seems to fit the data reasonably well. It appears that a rather simple interpolation between the two exponentials describes the intermediate range of durations ($0.5l' \leqslant l-\bar{l} \leqslant 1.2l'$) adequately.† Badri Narayanan *et al.* (1974, 1977) indicated that, across the entire boundary layer, l is distributed lognormally to a good approximation. The appropriate lognormal density evaluated from the measured values of $\bar{l}$ and l' is also plotted in the figure. Clearly, the lognormal is a reasonable fit only for relatively small l; the exponentials are a better overall fit to the data than the lognormal curve. Measurements at other Reynolds number ($6.8 \times 10^3 \leqslant R_\delta \leqslant 10^5$), not shown here,

† For random noise it appears that a single exponential describes adequately the entire range of l, with the exception of very small l.

confirm these conclusions. There are too few data points at very small l to say anything definite about $p(l)$ for that range.

Also marked in figure 13 are the inner and outer timescales ν/U_*^2 and δ/U_∞ respectively. (These are appropriately normalized by $\bar{l}$ and l'.) It is interesting to note that these numbers mark roughly the lower end of the respective regions of the two exponentials. If the long intervals are a consequence of large-scale structure passing the sensor, and the short intervals are a consequence largely of the nibbling small-scale motions superposed on large-scale structures, the above result means that both large- and small-scale structures are distributed exponentially. If the present interpretation is valid, kl', where k is the slope of the exponential tail in figure 13, should scale with the large-eddy timescale δ/U_∞. Because l' should also scale with δ/U as it gets a large contribution from the longer intervals l, k should be independent of Reynolds number. The inset to figure 13 shows that this is indeed so over the range covered in the experiments, giving strong support to the above conclusion.

5. Discussions and conclusions

Badri Narayanan *et al.* (1974, 1977) suggested that the zero-crossing scale is the most appropriate scaling parameter for the rate of occurrence of high-frequency pulses in turbulent velocity signals, and concluded that the vortex filaments represented by the high-frequency pulses have an average spacing of about 6 times the zero-crossing lengthscale. It is established here that they are based on erroneous measurements: the dissipation rate even of a non-Gaussian process is not far from that of a Gaussian process having the same mean number of zero-crossings. Zero-crossing measurements can be severely affected by factors like the dynamic range of the signal, noise content and the cut-off frequency; when those factors are not taken into account, misleading conclusions can easily be drawn. Present measurements show that the zero-crossing scale has in fact no more information than the Taylor microscale. In this important aspect, the somewhat speculative conclusions of Antonia *et al.* (1976) are consistent with the present measurements.

That the zero-crossing frequency is not equal to the pulse frequency of Rao *et al.* (1971) can be seen also as follows. First, N_0 varies significantly across the boundary layer (figure 10), while N_p measured by Rao *et al.* remains substantially independent of y/δ over a major part of the boundary layer. Further, we have shown that $U_\infty/N_0\delta \sim R_\theta^{-0.7}$, while Rao *et al.* and Ueda & Hinze (1975) found that $U_\infty/N_p\delta$ is a constant independent of the Reynolds number.

Rao *et al.* implied that the high-frequency pulses are associated with large structures, and the measurements of Brown & Thomas (1977) lend support to this implication. In general, when a large structure passes the sensor, we expect a zero-crossing interval of long duration. However, because of the small-scale fluctuations superposed on the large structures, it is plausible that a long zero-crossing interval is in general associated with a number of short runs at either end.† To obtain a rough estimate for this fraction, assume that the interval p.d.f. is made up entirely of exponentials. The fraction of zero-crossing due to the large scales alone is then given by the area under the exponential characterizing long intervals.

† Since a majority of the zero-crossing is really due to the small-scale motions, which are viscosity-dependent – even those short-duration intervals resulting when the large structures skim past the sensor are viscosity-dependent – the zero-crossing frequency to a large measure scales with the inner variables. The slight degree of Reynolds-number dependence shown in (4.2) must be due inevitably to the (small) fraction of long intervals caused by large structures.

Although, because of the intermediate region of l not covered by either exponential, there is some ambiguity in estimating the fractional area, a rough estimate shows that the area under this exponential is about 0.2 and, by implication, this also gives the ratio N_p/N_0 at this Reynolds number.

Two other points are worth a further look. First, this study has shown that $\Lambda/\lambda \approx 1$ for a wide variety of (but not necessarily all) strongly non-Gaussian signals. This opens up the possibility that Rice's result may be valid under a more general set of conditions which have nothing to do with the Gaussianity of the random process. Secondly, the fact that the zero-crossing intervals consist of a part easily identifiable with small-scale motion and a part with the large-scale motion suggests that a selective conditional sampling technique based on zero-crossings can be useful in separating the properties of large and small structures in turbulent shear flows.

We would like to acknowledge our many and long discussions with Prof. M. A. Badri Narayanan. K.R.S. would like to thank Dr D. Britz for his great help with the computations, and Prof. R. A. Antonia for generously making some of the laboratory equipment available for use in the experiments reported here. We also thank Drs B. G. Shivaprasad and B. N. S. Rao, and Messrs Ameenulla and N. S. Aswathanarayana Rao for the help rendered in making the experiments.

This work has been supported in part by ISRO through a sponsored project.

Appendix: Accuracy of zero-crossing measurements

In the present measurements, in addition to measuring the zero-crossing frequency from the recorded signals using a comparator/frequency-meter combination, visual counting and direct evaluation on a digital computer were also employed. In the latter method, all signals were pre-filtered† at the Kolmogorov frequency and digitized at twice the cut-off frequency, the basic idea being essentially that there is no 'signal' beyond the Kolmogorov frequency, and that the 'good' signal-to-noise ratio of the signals ensures that the noise contamination is negligible below the Kolmogorov frequency. All the signals were amplified sufficiently before digitizing, so as to suit the dynamic range of the A/D converter.

Table 3 gives a comparison between the values of N_0 obtained respectively by comparator and digital processing in a slightly heated axisymmetric jet. The data

	Jet axis		An intermittent position (intermittency factor ≈ 0.91)	
Signal	Comparator	Digital	Comparator	Digital
Axial velocity fluctuation u	310	309	260	250
Radial velocity fluctuation v	370	335	220	203
Temperature fluctuation θ	350	307	230	233

TABLE 3. Comparison of the zero-crossing frequency measured by comparator and digital processing

† As remarked towards the end of §3.3, cutting off at the Kolmogorov frequency does not automatically ensure that correct zero-crossing frequency will always be obtained. In addition, one generally has to make sure that there is a plateau region of the type discussed with respect to figure 6. This was indeed ensured here.

Comparator	Visual
196	211
285	305
362	369
470	454
555	527

TABLE 4. Comparison of the zero-crossing frequency obtained by comparator and visual methods

correspond to the flow studied by Antonia *et al.* (1976). Typically, the r.m.s. value of the digitized signals was of the order of 1–2 V. The 10 bit digitizer has a resolution of about 20 mV. Thus, the number of crossings counted will not be strictly those of zero, but of a band whose half-bandwidth is about 0.01–0.02 times the r.m.s. value of the signal. Then from figure 9, the digital values may be underestimating the true value of about 5 %. Even allowing for this error, it is clear that a difference of a few percent could exist between zero-crossing frequencies computed by those two different techniques. Differences of this order could arise because of the various other factors discussed in §3.

A comparison was also made of the zero-crossing frequency computed by the comparator and visual methods. In the visual method adopted here, the mean of the signal was first removed† and the signal amplified sufficiently (see §3.1) by passing it through a DISA 55D26 signal conditioner. Then, a large number of random samples of the signal was displayed on the oscilloscope and the zero-crossings counted. There is always some ambiguity in this technique because of the end-crossings on the oscilloscope screen. These were counted by the following (somewhat unsatisfactory) procedure. On either end of the screen, if a run appeared as if it had completed more than half its duration on the oscilloscope screen (as judged by its slope), it was consistently counted as a zero-crossing; otherwise, it was ignored. Obviously, this uncertainty decreases with increasing sweep time of the oscilloscope, because the total number of runs on the screen increases with increasing sweep time. However, the sweep time cannot be increased beyond a certain value because short runs then get so crowded together that they cannot easily be identified.

A comparison between the analogue and visual counting for wall shear stress fluctuations in a channel flow is shown in table 4 for increasing values of Reynolds number. It is interesting (although not necessarily significant) to note that the ratio comparator/visual crossing frequency increases from a value slightly less than unity to a value slightly greater than unity with increase in the numerical value of N_0. In all these cases, the sweep time in the visual method was the same; i.e. the number of runs/frame increased with increasing N_0. It appears that the simple rule used here of treating the end-crossings on the oscilloscope screen introduces an error which varies systematically with N_0.

It appears from this discussion that N_0 cannot be measured easily to an accuracy of better than *a few* percent.

† This fact was established by a real time-average performed using a box-car integrator.

REFERENCES

ANTONIA, R. A. 1973 *Phys. Fluids* **16**, 1198.

ANTONIA, R. A., DANH, H. Q. & PRABHU, A. 1976 *Phys. Fluids* **19**, 1680.

ANTONIA, R. A., DANH, H. Q. & PRABHU, A. 1977 *J. Fluid Mech.* **80**, 153.

ANTONIA, R. A., PRABHU, A. & STEPHENSON, A. 1975 *J. Fluid Mech.* **72**, 455.

BAKEWELL, H. P. & LUMLEY, J. L. 1976 *Phys. Fluids* **10**, 1880.

BATCHELOR, G. K. 1956 *The Theory of Homogeneous Turbulence.* Cambridge University Press.

BATCHELOR, G. K. & TOWNSEND, A. A. 1949 *Proc. R. Soc. Lond.* A **199**, 238.

BADRI NARAYANAN, M. A., RAJAGOPALAN, S. & NARASIMHA, R. 1974 Some experimental investigations of the fine structure of turbulence. *Rep.* 74 FM 15, *Dept Aero. Engng, Indian Inst. of Science.*

BADRI NARAYANAN, M. A., RAJAGOPALAN, S. & NARASIMHA, R. 1977 *J. Fluid Mech.* **80**, 237.

BLACKWELDER, R. F. & KOVASZNAY, L. S. G. 1970 Large scale motion of a turbulent boundary layer with a zero and a favourable pressure gradient. *Interim Tech. Rep., Dept Mech., The Johns Hopkins University.*

BOWEN, R. 1970 *Proc. Symp. Pure Math.* **14**, 23.

BROWN, G. L. & THOMAS, A. S. W. 1977 *Phys. Fluids Suppl.* **20**, S243.

CLAUSER, F. 1955 *Adv. Appl. Mech.* **4**, 1.

COMTE-BELLOT, G. 1963 Ph.D. thesis, Univ. of Grenoble [English transl. by P. Bradshaw, *ARC* FM 4102 (1969)].

FELLER, W. 1957 *An Introduction to Probability Theory and its Applications.* Wiley.

GUPTA, A. K. & KAPLAN, R. E. 1972 *Phys. Fluids* **15**, 981.

KLEBANOFF, P. S. 1955 Characteristics of turbulence in a boundary layer with zero pressure gradient. *NACA TR* 1247.

KLINE, S. J., REYNOLDS, W. C., SCHRAUB, F. A. & RUNSTADLER, P. W. 1967 *J. Fluid Mech.* **30**, 741.

KUO, A. S. & CORRSIN, S. 1971 *J. Fluid Mech.* **50**, 285.

KUZNETSOV, P. L., STRATONOVICH, R. L. & TIKNONOV, V. I. 1954 *J. Tech. Phys., Moscow* **24**, 103.

LAUFER, J. 1950 *J. Aero. Sci.* **17**, 277.

LIEPMANN, H. W. 1949 *Helv. Phys. Acta* **22**, 119.

LIEPMANN, H. W., LAUFER, J. C. & LIEPMANN, K. 1951 On the spectrum of isotropic turbulence. *NACA TN* 2473.

LONGUET-HIGGINS, M. S. 1958 *Proc. R. Soc. Lond.* A **246**, 99.

RAO, K. N., NARASIMHA, R. & BADRI NARAYANAN, M. A. 1971 *J. Fluid Mech.* **48**, 339.

REPIK, YE. U. & SOSEDKO, YU. P. 1976 *Fluid Mech.–Sov. Res.* **5**, 39.

RICE, S. O. 1945 *Bell Syst. Tech. J.* **24**, 46.

SREENIVASAN, K. R. 1983 Submitted for publication.

SREENIVASAN, K. R., ANTONIA, R. A. & DANH, H. Q. 1977 *Phys. Fluids* **20**, 1800.

TOWNSEND, A. A. 1951 *Proc. Camb. Phil. Soc.* **47**, 375.

UEDA, H. & HINZE, J. O. 1975 *J. Fluid Mech.* **67**, 125.

WETZEL, J. M. & KILLEN, J. M. 1972 A preliminary report on the zero-crossing rate technique for average shear measurement in flowing fluid. *Rep.* 134, *Univ. Minnesota, St Anthony Falls Hydraulics Lab.*

WYGNANSKI, I. & FIEDLER, H. 1969 *J. Fluid Mech.* **38**, 577.

YLVISAKER, N. D. 1965 *Ann. Math. Stat.* **36**, 1043.